Original Article

Dynamic Alterations in Microarchitecture, Mineralization and Mechanical Property of Subchondral Bone in Rat Medial Meniscal Tear Model of Osteoarthritis

De-Gang Yu[1], Shao-Bo Nie[2], Feng-Xiang Liu[1], Chuan-Long Wu[1], Bo Tian[1], Wen-Gang Wang[1], Xiao-Qing Wang[1], Zhen-An Zhu[1], Yuan-Qing Mao[1]

[1]Shanghai Key Laboratory of Orthopedic Implants, Department of Orthopaedic Surgery, Shanghai Ninth People's Hospital, Shanghai Jiao Tong University School of Medicine, Shanghai 200011, China

[2]Department of Orthopaedic Surgery, Chinese People's Liberation Army General Hospital, Beijing 100853, China

De-Gang Yu and Shao-Bo Nie contributed equally to this work.

Abstract

Background: The properties of subchondral bone influence the integrity of articular cartilage in the pathogenesis of osteoarthritis (OA). However, the characteristics of subchondral bone alterations remain unresolved. The present study aimed to observe the dynamic alterations in the microarchitecture, mineralization, and mechanical properties of subchondral bone during the progression of OA.

Methods: A medial meniscal tear (MMT) operation was performed in 128 adult Sprague Dawley rats to induce OA. At 2, 4, 8, and 12 weeks following the MMT operation, cartilage degeneration was evaluated using toluidine blue O staining, whereas changes in the microarchitecture indices and tissue mineral density (TMD), mineral-to-collagen ratio, and intrinsic mechanical properties of subchondral bone plates (BPs) and trabecular bones (Tbs) were measured using micro-computed tomography scanning, confocal Raman microspectroscopy and nanoindentation testing, respectively.

Results: Cartilage degeneration occurred and worsened progressively from 2 to 12 weeks after OA induction. Microarchitecture analysis revealed that the subchondral bone shifted from bone resorption early (reduced trabecular BV/TV, trabecular number, connectivity density and trabecular thickness [Tb.Th], and increased trabecular spacing (Tb.Sp) at 2 and 4 weeks) to bone accretion late (increased BV/TV, Tb.Th and thickness of subchondral bone plate, and reduced Tb.Sp at 8 and 12 weeks). The TMD of both the BP and Tb displayed no significant changes at 2 and 4 weeks but decreased at 8 and 12 weeks. The mineral-to-collagen ratio showed a significant decrease from 4 weeks for the Tb and from 8 weeks for the BP after OA induction. Both the elastic modulus and hardness of the Tb showed a significant decrease from 4 weeks after OA induction. The BP showed a significant decrease in its elastic modulus from 8 weeks and its hardness from 4 weeks.

Conclusion: The microarchitecture, mineralization and mechanical properties of subchondral bone changed in a time-dependent manner as OA progressed.

Key words: Mechanical Property; Microarchitecture; Mineralization; Osteoarthritis; Subchondral Bone

Introduction

Osteoarthritis (OA), a leading cause of disability in the elderly,[1] is characterized by the progressive loss of articular cartilage, the formation of subchondral bone lesions, and a slight synovial reaction.[2] For decades, the role of subchondral bone has been largely ignored, as alterations in the subchondral bone were generally considered to occur secondarily to cartilage degeneration.[3,4] However, recent data have demonstrated that an impaired subchondral bone

Access this article online

Quick Response Code:

Website: www.cmj.org

DOI: 10.4103/0366-6999.168045

Address for correspondence: Dr. Yuan-Qing Mao, Shanghai Key Laboratory of Orthopaedic Implants, Department of Orthopaedic Surgery, Shanghai Ninth People's Hospital, Shanghai Jiao Tong University School of Medicine, 639 Zhizaoju Road, Shanghai 200011, China
E-Mail: doctormaoyuanqing@126.com

Received: 31-03-2015 **Edited by:** Li-Shao Guo

How to cite this article: Yu DG, Nie SB, Liu FX, Wu CL, Tian B, Wang WG, Wang XQ, Zhu ZA, Mao YQ. Dynamic Alterations in Microarchitecture, Mineralization and Mechanical Property of Subchondral Bone in Rat Medial Meniscal Tear Model of Osteoarthritis. Chin Med J 2015;128:2879-86.

can aggravate the degeneration of the overlying cartilage and an improved subchondral bone can retard cartilage degeneration,[5-10] which indicates that the properties of subchondral bone influence the integrity of articular cartilage in the pathogenesis of OA. From the biomechanical point of view, articular cartilage contains a lot of water and has a strong capacity to withstand compressive stress but has weak capacities to withstand tensile and shear stress. Heterogeneities in the density and rigidity of subchondral bone in OA, along with mutated material composition and disorganized microstructure, result in abnormal tensile stress and shear stress toward articular cartilage, thus facilitating cartilage degeneration. However, the characteristics of subchondral bone alterations remain unresolved, and a better understanding of these alterations may contribute to the development of bone-targeting therapies.

Clinical data have demonstrated that osteoarthritic subchondral bone turnover increases dramatically,[6,11] which results in disorganized bone architecture, decreased mineralization, and weakened biomechanical properties.[12-14] Subchondral osteoblasts and osteoclasts manifest abnormal functions,[15,16] producing various cytokines, growth factors, prostaglandins, and leukotrienes, which could accelerate cartilage degradation.[17] However, most of these studies were focused on end-stage disease, which reveals little about early deregulation of bone turnover.

Many animal models have been developed to study the pathophysiology of OA and to evaluate potential therapeutics.[18,19] Alterations in the subchondral bone have been detected with dual-energy X-ray absorptiometry,[20,21] histomorphometry,[21-24] or micro-computed tomography (micro-CT).[9,25,26] These changes include increased bone resorption in the early stage of OA, indicated as reduced bone mineral density (BMD), bone volume, trabecular thickness (Tb.Th) and connectivity, and increased bone accretion later in the disease, with increases in bone volume and Tb.Th, decreases in trabecular number (Tb.N) and separation, and subchondral sclerosis.

However, bone is a complex tissue, the principal function of which is to resist mechanical forces, with its overall properties depending not only on quantity but also on quality, as characterized by its architecture, material composition (mineral and collagen), and intrinsic mechanical properties.[27,28] Presently, there is no report on the alterations in the overall properties of subchondral bone during OA progression. Confocal Raman spectroscopy systems, which are capable of probing the physiochemical properties of bone tissue based on the ratios of relative Raman peak intensity generated by the mineral and collagen phases,[29] has been used to evaluate the mineral-to-collagen ratio of bone in recent years. Nanoindentation, which emerged as a powerful tool for measuring the mechanical properties of small and complex biomaterials, has been used to investigate variations in the mechanical properties of trabecular and cortical bone in osteoporosis.[30,31] Thus, using histology, micro-CT, Raman spectroscopy and nanoindentation, the current study observed the potential changes in the microarchitecture, tissue mineral density (TMD), mineral-to-collagen ratio, and intrinsic mechanical properties to evaluate the properties of subchondral bone in the commonly used rat medial meniscal tear (MMT) model of OA.

Methods

Animals

Adult male Sprague Dawley rats (12 weeks old, weighing 276 ± 16 g) from Sino-British Sippr/BK Lab Animal Ltd., (Shanghai, China) were used in the present study. The animals were group housed under a 12-h light/dark cycle with food and water provided *ad libitum*. The animals received standard laboratory chow containing 1.56% calcium, 0.8% phosphorus, and 800 IU/kg Vitamin D. The Animal Care and Experiment Committee of Shanghai Jiao Tong University School of Medicine approved all experimental procedures.

Induction of osteoarthritis and experimental design

The rats were anesthetized with 10% chloral hydrate in phosphate-buffered saline (0.01 mol/L) after 1 week of acclimatization. The MMT model was induced as previously described.[32] Briefly, the medial collateral ligament of the right knee was transected, and the medial meniscus was reflected proximally toward the femur and cut through at its narrowest point. For the controls (Sham), the wounds were closed after exposing the medial collateral ligament. A total of 128 animals (64 for MMT and Sham groups, respectively) were used to observe changes in cartilage and subchondral bone. Animals were sacrificed at 2, 4, 8, and 12 weeks after the operation.

Tissue preparation

The entire knee joint was dissected and fixed in 4% paraformaldehyde for 48 h. Eight joints from each group at every time point were decalcified in 10% ethylenediaminetetraacetic acid for 3 weeks. The joints were then bisected along the collateral ligament in the frontal plane, and both sections were embedded in the same paraffin block. The samples were cut into 5-μm sections and prepared for toluidine blue O staining to evaluate cartilage degeneration. The other 8 undecalcified joints from the Sham and MMT groups at each time point were used to evaluate the properties of subchondral bone, including micro-CT imaging, confocal Raman microspectroscopy, and nanoindentation.

Histological analysis

On the basis of the Osteoarthritis Research Society International (OARSI) recommendations for the histological assessment of OA in the rat,[33] 3 sections from each knee at 200-mm steps were stained with toluidine blue O and subsequently evaluated for cartilage degeneration. For toluidine blue O staining, the sections were stained with 0.04% w/v toluidine blue O (Sigma, T0394, USA) in 0.1 mol/L sodium acetate (pH 4.0) for 10 min, rinsed briefly, air-dried and mounted. The medial tibial plateau was divided into three regions of equal width, and cartilage degeneration in each zone was scored "none" to "severe" (numerical values 0–5) using the criteria described in Table 1. The original surface of the tissue was estimated. Then,

the percentage area of each zone containing cartilage exhibiting loss of chondrocytes or loss of matrix was estimated, and a score was assigned to that zone based on that percentage. The total cartilage degeneration score was calculated by adding the values obtained for each zone.

Micro-computed tomography imaging and analysis

Structural alterations and the tissue mineral content in the subchondral bone were evaluated using micro-CT. The knee joints were scanned by micro-CT (μCT 80; Scanco Medical AG, Bassersdorf, Switzerland) with an isotropic voxel resolution of 10 μm. As shown in our previous study,[34] a portion (2.0 mm ventrodorsal length) of the load-bearing region at the medial tibial plateau was identified as a region of interest [Figure 1]. Both subchondral bone plate (BP) and trabecular bone (Tb) parameters were calculated.

Confocal Raman microspectroscopy

The chemical composition of the subchondral bone tissue (mineral-to-collagen ratio, υ_1-PO_4^{3-}/proline) was characterized by confocal Raman microspectroscopy (Renishaw Inc., Hoffman Estates, IL, USA) as described previously.[8,35] After micro-CT scanning, joint samples were dehydrated in a graded alcohol series, embedded in methyl methacrylate (MMA) and sliced in the frontal plane using a Leica SP1600 saw microtome. The section surface was ground on successive grits of wet silicon carbide paper and polished by hand with 1 μm alumina slurry, and 3 sections of 30 μm thickness from each sample were obtained and analyzed. A 50X objective focused the laser (785 nm laser diode source) on a 3 μm region within the medial tibial plateau, and Raman scattered light was collected by a spectrograph with 0.5 cm^{-1} spectral resolution. The measured spectra consisted of three accumulations with an integration time of 10 s each. Using custom-developed software (MATLAB, MathWorks, Natick, MA, USA), the background fluorescence in the spectra was subtracted by a modified polynomial fitting algorithm.[36] Underlying the regions of articular cartilage damage, spectra were collected from three locations within the subchondral BP and eight locations within the Tb. The υ_1-PO_4^{3-}/proline ratio was then calculated as the raw υ_1 phosphate peak intensity (υ_1-PO_4^{3-}, 962 cm^{-1}) per proline peak intensity (856 cm^{-1}) and averaged per section.

Table 1: Osteoarthritis Research Society International recommended cartilage degeneration score for rats

Grade	Description
0	No degeneration
1	Minimal degeneration; 5–10% of the total projected cartilage area affected by matrix or chondrocyte loss
2	Mild degeneration; 11–25% affected
3	Moderate degeneration; 26–50% affected
4	Marked degeneration; 51–75% affected
5	Severe degeneration; >75% affected

Nanoindentation testing

The mechanical properties at the tissue level were quantified by nanoindentation as described previously.[37] Following the confocal Raman microspectroscopy, the medial tibial plateau of MMA-embedded knee sections were probed using a TriboIndenter (Hysitron Inc., Minneapolis, MN, USA). A Berkovitch diamond tip (inclination angle 142.35°, radius 200 nm) was pressed into the surface using a trapezoidal loading scheme as follows: (1) Loading up to a nominal load of 1000 μN at a rate of 200 μN/s; (2) holding at Pmax for 5 s; and (3) unloading to zero load at a rate of 200 μN/s. Thermal drift was corrected in the measurement software (Triboscan) by measuring the indenter drift for a maximum of 40 s before the start of every indent and applying this correction to the measured data. From the resulting force-displacement curve, the elastic modulus (E_r) and hardness (H) of the tissue at the point of indention (0.25 μm resolution) was calculated following the method of Oliver and Pharr.[38] Underlying the regions of articular cartilage damage, three locations on BP and eight locations on Tb per section were chosen, and four indents for each location were tested and averaged per section.

Statistical analysis

All of the statistical analyses were performed by blinded authors who were unaware of the treatments given. The results were presented as the mean ± standard deviation (SD). A comparison between the Sham and MMT groups was performed with an independent-samples *t*-test. $P < 0.05$ was considered statistically significant. Statistical analysis was conducted with SPSS for Windows, version 11.5 (SPSS Inc., Chicago, IL, USA).

Results

Articular cartilage degeneration

As indicated by toluidine blue O staining [Figure 2], MMT induced cartilage degeneration primarily on the

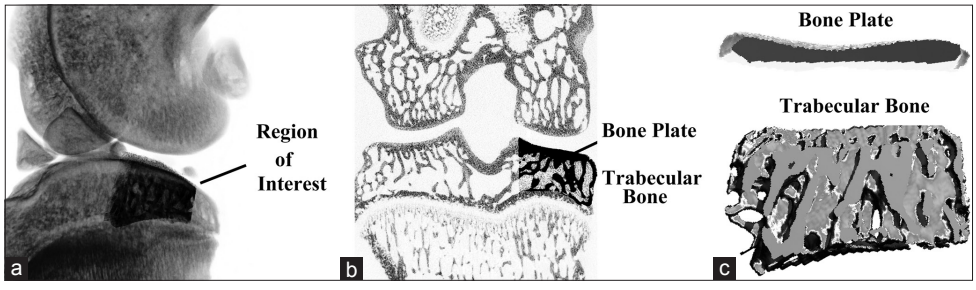

Figure 1: Schematic of the micro-computed tomography analysis. (a) A portion of 2.0 mm ventrodorsal length at the medial tibial plateau was identified as a region of interest; (b and c) Alterations in the subchondral bone plate and trabecular bone were calculated, respectively.

outer regions of the medial tibia platform. Cartilage matrix and chondrocyte loss occurred and worsened in a time-dependent manner from 2 to 12 weeks postsurgery, whereas the Sham joints showed no obvious changes at any time point. At 2 weeks, matrix and chondrocyte loss mainly affected the superficial and upper middle zone. Subsequently, these changes reached the deep zone and extended more substantially into the medial tibial plateau at 4 weeks. Severe degeneration occurred at 8 weeks with full thickness involvement into the tidemark, which became more widespread at 12 weeks. Specifically, the cartilage degeneration scores for the MMT joints were 3.60 ± 0.52, 6.33 ± 0.74, 9.18 ± 1.13, and 12.85 ± 1.36 at 2, 4, 8, and 12 weeks, respectively.

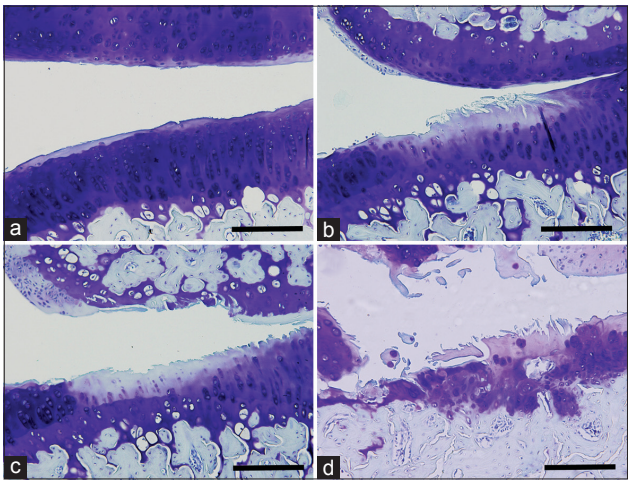

Figure 2: Changes in articular cartilage during osteoarthritis progression. Representative images with toluidine blue O staining. (a-d) Joints harvested at 2, 4, 8, and 12 weeks after medial meniscal tear operation. Bar = 200 μm.

Changes in subchondral bone microarchitecture and tissue mineral density

Representative pictures of the knee joints from Sham and MMT groups obtained by micro-CT scanning are shown in Figure 3. In general, subchondral bone of the medial tibial plateau showed dynamic alterations following OA induction from bone resorption at the early stages (2 and 4 weeks) to bone accretion at the advanced stages (8 and 12 weeks). Specifically, compared with

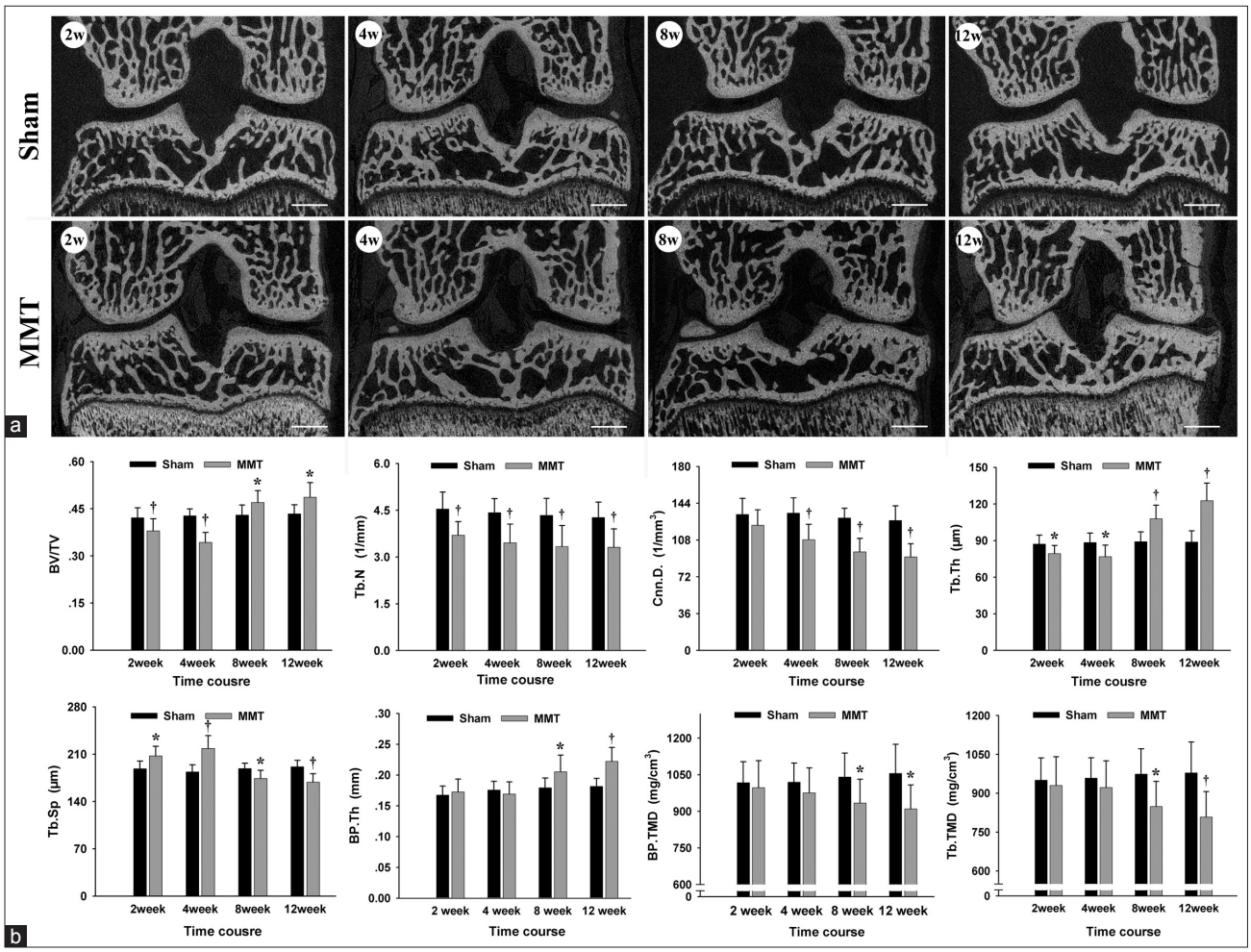

Figure 3: Changes in subchondral bone microarchitecture and tissue mineral density (a) Representative images of the knee obtained with micro-computed tomography scanning, Bar = 1000 μm. (b) Analysis of subchondral bone microstructure parameters and tissue mineral density. n = 8/group. Mean ± standard deviation. *P < 0.05 and †P < 0.01, compared with Sham group.

the Sham groups, the thickness of subchondral bone plate (BP.Th) in the MMT groups showed no significant changes at 2 and 4 weeks ($P > 0.05$, respectively), but increased significantly at 8 and 12 weeks ($P < 0.05$ and $P < 0.01$, respectively). The bone volume fraction (BV/TV) of Tb decreased at 2 and 4 weeks ($P < 0.01$, respectively) and increased at 8 and 12 weeks ($P < 0.05$, respectively). These changes were accompanied by the Tb.Th changing from thinner (2 and 4 weeks, $P < 0.05$, respectively) to thicker (8 and 12 weeks, $P < 0.01$, respectively), the trabecular spacing (Tb.Sp) from broader (2 and 4 weeks, $P < 0.05$ and $P < 0.01$, respectively) to narrower (8 and 12 weeks, $P < 0.05$ and $P < 0.01$, respectively), and the Tb.N and connectivity density (Cnn.D) being reduced at all times ($P < 0.01$). With respect to TMD, compared with the Sham groups, both the subchondral BP and Tb displayed no significant changes at 2 and 4 weeks ($P > 0.05$, respectively), but decreased at 8 and 12 weeks ($P < 0.05$, respectively).

Changes in subchondral bone mineral-to-collagen ratio

The mineral-to-collagen ratio of the subchondral bone tissue, calculated as the υ_1-PO_4^{3-} peak intensity per proline peak intensity ($PO4^{3-}$/proline) using confocal Raman microspectroscopy, is shown in Figure 4. In general, no significant difference in mineral-to-collagen ratio was observed among the Sham groups, whereas, a reduced mineral-to-collagen ratio was found in MMT animals that were aggravated with the progression of the disease. Specifically, the mineral-to-collagen ratio of the subchondral BP in MMT animals was reduced from 10.14 ± 1.94 at 2 weeks to 8.21 ± 1.45 at 12 weeks. Simultaneously, the mineral-to-collagen ratio of the Tb in MMT animals was reduced from 9.09 ± 1.97 at 2 weeks to 6.66 ± 1.43 at 12 weeks.

Changes in intrinsic bone mechanical properties

The intrinsic bone tissue mechanical properties, displayed as elastic modulus E_r and hardness H quantified by nanoindentation, are shown in Figures 5 and 6. The mechanical properties of the subchondral bone in the Sham groups showed no significant changes throughout the course of the experiment, whereas the mechanical properties of subchondral bone in the MMT groups were gradually reduced as the disease progressed following the MMT operation. Specifically, the elastic modulus of the subchondral BP in MMT animals was reduced from 21.75 ± 3.64 GPa at 2 weeks to 17.41 ± 3.88 GPa at 12 weeks, whereas the hardness was reduced from 0.96 ± 0.13 GPa at 2 weeks to 0.76 ± 0.13 GPa at 12 weeks. With respect to the Tb, the elastic modulus in MMT animals was reduced from

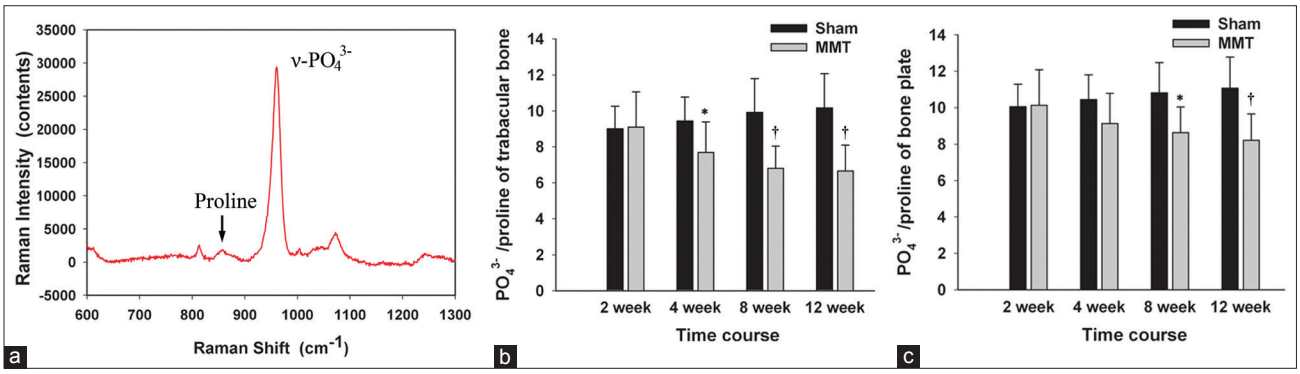

Figure 4: Changes in the mineral-to-collagen ratio of the subchondral bone plate and trabecular bone. (a) A typical Raman spectrum from the subchondral bone. The mineral-to-collagen ratio ($\upsilon 1$-PO_4^{3-}/proline) was calculated as the raw $\upsilon 1$ phosphate peak intensity ($\upsilon 1$-PO_4^{3-}, 962 cm^{-1}) per proline peak intensity (856 cm^{-1}). (b) $\upsilon 1$-PO_4^{3-}/proline of the subchondral trabecular bone. (c) $\upsilon 1$-PO_4^{3-}/proline of the subchondral bone plate. n = 8/group. Mean ± standard deviation. *$P < 0.05$ and †$P < 0.01$, compared with Sham group.

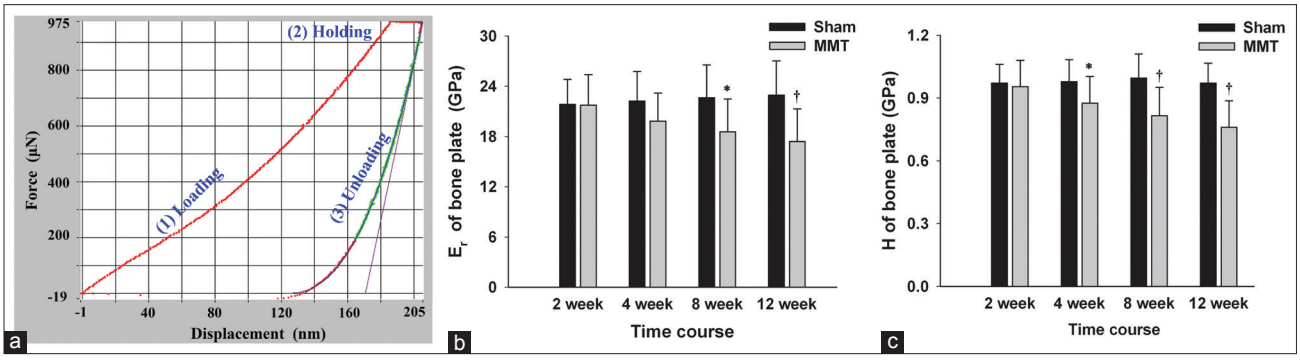

Figure 5: Intrinsic mechanical properties of the subchondral bone plate. (a) Representative nanoindentation load-displacement curve from the subchondral bone plate. The Er and H of the tissue at the point of indention were calculated following the method of Oliver and Pharr. (b and c) Er and H of the subchondral bone plate. n = 8/group. Mean ± standard deviation. *$P < 0.05$ and †$P < 0.01$, compared with Sham group, Er: Elastic modulus; H: Hardness.

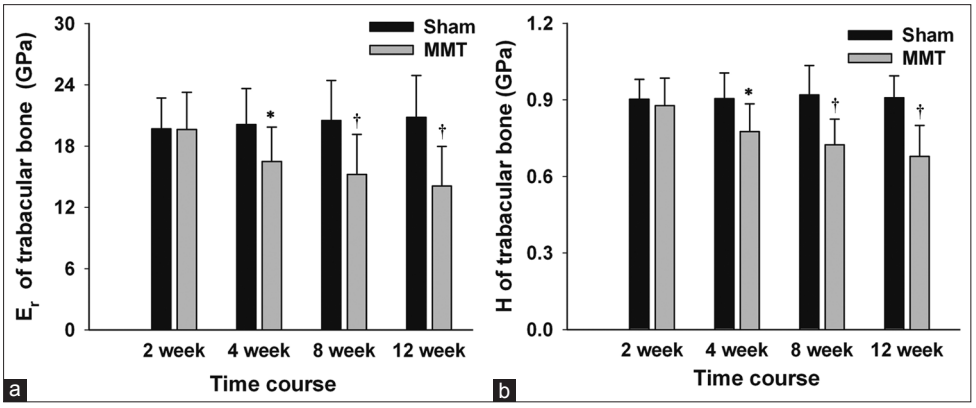

Figure 6: Intrinsic mechanical properties of subchondral trabecular bone. (a) Er of subchondral trabecular bone. (b) H of subchondral trabecular bone. n = 8/group. Mean ± standard deviation. *P < 0.05 and †P < 0.01, compared with Sham group, Er: Elastic modulus; H: Hardness.

19.62 ± 3.64 GPa at 2 weeks to 14.08 ± 3.88 GPa at 12 weeks, whereas the hardness was reduced from 0.88 ± 0.11 GPa at 2 weeks to 0.68 ± 0.12 GPa at 12 weeks.

Discussion

The rat MMT model is well-established and commonly used to study the pathophysiology of OA and to evaluate potential therapeutics.[19,33] Consistent with previous results,[33] the present study demonstrated that cartilage degeneration and subchondral alterations occurred in a time-dependent manner in the rat MMT model. Bone resorption dominates the early stage of disease, manifested as a decreased BV/TV ratio, reduced Tb.N and Cnn.D, thinned Tb.Th, and broadened Tb.Sp. With the progression of the disease, bone alterations shift from bone resorption to a bone formation at an advanced stage, manifested as increased BV/TV ratio, thickened Tb.Th and narrowed Tb.Sp.

Bone is a complex tissue, its overall properties depending not only on quantity, as manifested by BMD and BV/TV, but also on quality, as embodied in TMD, architecture, material composition, and mechanical properties.[27,28] For the first time, the present study observed the changes in the material composition and mechanical properties of subchondral bone in a rat MMT model of OA. Our data revealed that both the subchondral BP and Tb demonstrated a gradually reduced mineral-to-collagen ratio, elastic modulus and hardness with the progression of the disease. Consistent with our findings, a subchondral bone from patients with late OA showed decreased mineralization.[12,39] The potential mechanism by which mineralization and mechanical properties were reduced may lie in the increased bone turnover of the osteoarthritic subchondral bone.[13,40] Bone turnover, which is mediated by osteoclast-osteoblast coupling as the main biological determinant of bone mineralization, increases dramatically in the pathogenesis of OA.[41] This accounts for much of the bone that lacked an opportunity to fully mineralize, resulting in the corresponding reduction of mechanical properties. Due to reduced intrinsic mechanical properties, subchondral osteoblast enhanced anabolic activity, and increased bone formation[15] to bear abnormal joint stress,[42] which led to an increased BV/TV ratio, thickened BP and Tb.Th, and narrowed Tb.Sp. Consequently, incomplete mineralization, reduced intrinsic mechanical properties, increased bone formation and abnormal joint stress contribute together to flattening, depression and sclerosis of the articular surface, which can be observed on radiographs or magnetic resonance imaging.

Subchondral bone consists of the corticalized BP and the underlying Tb.[43] Inconsistent results with respect to the BP.Th in OA were obtained in previous studies. Samples from patients with late OA displayed thickened subchondral BPs.[13] In animal experiments, some observed a thinned subchondral BP,[44-46] whereas others observed a thickened subchondral BP.[24,47,48] The current study demonstrated that the BP.Th showed no obvious difference at the early stage but found thickening at the late stage in the rat MMT model. The inconsistency may be attributed to the adoption of different animal models or measurements and/or differences in the time points or stages of disease progression observed. The subchondral BP and Tb showed similar trends in TMD, the mineral-to-collagen ratio and mechanical properties with the progression of disease in the present MMT model. Compared with the BP, the Tb changed earlier and more obviously, similar to the phenomenon in osteoporosis when Tb shows more obvious changes than cortical bone owing to the high bone turnover rate in Tb.[49]

The precise causes leading to dynamic alterations in subchondral bone with disease progression remain unknown. The possible mechanisms of increased subchondral bone remodeling in early OA may include repair of microscopic damage,[50,51] vascular invasion induced by pro-angiogenic factors,[52] and bone and cartilage interactions through micropores[53] in the subchondral bone. While the mechanisms, by which subchondral bone mineralization is reduced in late OA may be related to osteoblast differentiation factors.[54]

It has been shown that interaction between bone and cartilage is strengthened in OA,[46,53] and the subchondral osteoblasts, osteoclasts in OA can release a variety of proteases, inflammatory mediators, and growth factors

that can promote chondrocyte death in the upper layer and matrix degradation.[17] However, the present study only observed subchondral changes in the biomechanical point of view. Further study of subchondral bone is needed from the aspect of molecular biology. Finally, the present findings may have some implications for the treatment of OA with bone-modifying agents. Previous preclinical studies have revealed that targeting subchondral bone with bone-modifying agents,[8,23,55,56] such as the anti-bone resorption drugs of estrogen, calcitonin, bisphosphonates and OPG, the pro-osteogenesis drug teriparatide, and the bidirectional regulation drug strontium ranelate, has protective effects on osteoarthritic articular cartilage, and a number of clinical trial results also support the positive roles of osteoprotective agents in inhibiting the degradation of cartilage type II collagen and delaying cartilage degeneration in OA.[57-59] However, these protective effects have not been consistently confirmed by clinical data.[41,60] The present findings that the properties of subchondral bone are dynamic with disease progression indicate that abnormal subchondral bone cannot always be modified, and the stage of disease progression may influence the efficacy of bone-modifying therapy.

In conclusion, alterations in the bone volume, microarchitecture, TMD, mineral-to-collagen ratio, and intrinsic mechanical properties of subchondral bone change in a time-dependent manner as the disease progresses in the rat MMT model of OA.

Financial support and sponsorship

This work was supported by grants from the National Natural Science Foundation of China (No. 81272036 and No. 81301590) and Sectors Fund Project of the Ministry of Health of China (No. 201302007).

Conflicts of interest

There are no conflicts of interest.

References

1. Holman HR, Lorig KR. Overcoming barriers to successful aging. Self-management of osteoarthritis. West J Med 1997;167:265-8.
2. Lane NE, Brandt K, Hawker G, Peeva E, Schreyer E, Tsuji W, *et al.* OARSI-FDA initiative: Defining the disease state of osteoarthritis. Osteoarthritis Cartilage 2011;19:478-82.
3. Felson DT, Neogi T. Osteoarthritis: Is it a disease of cartilage or of bone? Arthritis Rheum 2004;50:341-4.
4. Mansell JP, Collins C, Bailey AJ. Bone, not cartilage, should be the major focus in osteoarthritis. Nat Clin Pract Rheumatol 2007;3:306-7.
5. Karsdal MA, Leeming DJ, Dam EB, Henriksen K, Alexandersen P, Pastoureau P, *et al.* Should subchondral bone turnover be targeted when treating osteoarthritis? Osteoarthritis Cartilage 2008;16:638-46.
6. Kwan Tat S, Lajeunesse D, Pelletier JP, Martel-Pelletier J. Targeting subchondral bone for treating osteoarthritis: What is the evidence? Best Pract Res Clin Rheumatol 2010;24:51-70.
7. Bellido M, Lugo L, Roman-Blas JA, Castañeda S, Calvo E, Largo R, *et al.* Improving subchondral bone integrity reduces progression of cartilage damage in experimental osteoarthritis preceded by osteoporosis. Osteoarthritis Cartilage 2011;19:1228-36.
8. Yu DG, Ding HF, Mao YQ, Liu M, Yu B, Zhao X, *et al.* Strontium ranelate reduces cartilage degeneration and subchondral bone remodeling in rat osteoarthritis model. Acta Pharmacol Sin 2013;34:393-402.
9. Bellido M, Lugo L, Roman-Blas JA, Castañeda S, Caeiro JR, Dapia S, *et al.* Subchondral bone microstructural damage by increased remodelling aggravates experimental osteoarthritis preceded by osteoporosis. Arthritis Res Ther 2010;12:R152.
10. Cox LG, van Rietbergen B, van Donkelaar CC, Ito K. Bone structural changes in osteoarthritis as a result of mechanoregulated bone adaptation: A modeling approach. Osteoarthritis Cartilage 2011;19:676-82.
11. Goldring SR. Role of bone in osteoarthritis pathogenesis. Med Clin North Am 2009;93:25-35, xv.
12. Li B, Aspden RM. Composition and mechanical properties of cancellous bone from the femoral head of patients with osteoporosis or osteoarthritis. J Bone Miner Res 1997;12:641-51.
13. Bailey AJ, Mansell JP, Sims TJ, Banse X. Biochemical and mechanical properties of subchondral bone in osteoarthritis. Biorheology 2004;41:349-58.
14. Burr DB. Anatomy and physiology of the mineralized tissues: Role in the pathogenesis of osteoarthrosis. Osteoarthritis Cartilage 2004;12 Suppl A: S20-30.
15. Sanchez C, Deberg MA, Bellahcène A, Castronovo V, Msika P, Delcour JP, *et al.* Phenotypic characterization of osteoblasts from the sclerotic zones of osteoarthritic subchondral bone. Arthritis Rheum 2008;58:442-55.
16. Chan TF, Couchourel D, Abed E, Delalandre A, Duval N, Lajeunesse D. Elevated Dickkopf-2 levels contribute to the abnormal phenotype of human osteoarthritic osteoblasts. J Bone Miner Res 2011;26:1399-410.
17. Prasadam I, van Gennip S, Friis T, Shi W, Crawford R, Xiao Y. ERK-1/2 and p38 in the regulation of hypertrophic changes of normal articular cartilage chondrocytes induced by osteoarthritic subchondral osteoblasts. Arthritis Rheum 2010;62:1349-60.
18. Bendele AM. Animal models of osteoarthritis. J Musculoskelet Neuronal Interact 2001;1:363-76.
19. Poole R, Blake S, Buschmann M, Goldring S, Laverty S, Lockwood S, *et al.* Recommendations for the use of preclinical models in the study and treatment of osteoarthritis. Osteoarthritis Cartilage 2010;18 Suppl 3:S10-6.
20. Doschak MR, Wohl GR, Hanley DA, Bray RC, Zernicke RF. Antiresorptive therapy conserves some periarticular bone and ligament mechanical properties after anterior cruciate ligament disruption in the rabbit knee. J Orthop Res 2004;22:942-8.
21. Wang SX, Laverty S, Dumitriu M, Plaas A, Grynpas MD. The effects of glucosamine hydrochloride on subchondral bone changes in an animal model of osteoarthritis. Arthritis Rheum 2007;56:1537-48.
22. Hayami T, Pickarski M, Zhuo Y, Wesolowski GA, Rodan GA, Duong le T. Characterization of articular cartilage and subchondral bone changes in the rat anterior cruciate ligament transection and meniscectomized models of osteoarthritis. Bone 2006;38:234-43.
23. Hayami T, Pickarski M, Wesolowski GA, McLane J, Bone A, Destefano J, *et al.* The role of subchondral bone remodeling in osteoarthritis: Reduction of cartilage degeneration and prevention of osteophyte formation by alendronate in the rat anterior cruciate ligament transection model. Arthritis Rheum 2004;50:1193-206.
24. Fahlgren A, Messner K, Aspenberg P. Meniscectomy leads to an early increase in subchondral bone plate thickness in the rabbit knee. Acta Orthop Scand 2003;74:437-41.
25. Boyd SK, Müller R, Zernicke RF. Mechanical and architectural bone adaptation in early stage experimental osteoarthritis. J Bone Miner Res 2002;17:687-94.
26. McErlain DD, Appleton CT, Litchfield RB, Pitelka V, Henry JL, Bernier SM, *et al.* Study of subchondral bone adaptations in a rodent surgical model of OA using *in vivo* micro-computed tomography. Osteoarthritis Cartilage 2008;16:458-69.
27. Viguet-Carrin S, Garnero P, Delmas PD. The role of collagen in bone strength. Osteoporos Int 2006;17:319-36.
28. Seeman E, Delmas PD. Bone quality – The material and structural basis of bone strength and fragility. N Engl J Med 2006;354:2250-61.
29. Nyman JS, Makowski AJ, Patil CA, Masui TP, O'Quinn EC, Bi X, *et al*. Measuring differences in compositional properties of bone tissue by confocal Raman spectroscopy. Calcif Tissue Int 2011; 89:111-22.
30. Ebenstein DM, Pruitt LA. Nanoindentation of biological materials. Nano Today 2006;1:26-33.

31. Lewis G, Nyman JS. The use of nanoindentation for characterizing the properties of mineralized hard tissues: State-of-the art review. J Biomed Mater Res B Appl Biomater 2008;87:286-301.
32. Janusz MJ, Bendele AM, Brown KK, Taiwo YO, Hsieh L, Heitmeyer SA. Induction of osteoarthritis in the rat by surgical tear of the meniscus: Inhibition of joint damage by a matrix metalloproteinase inhibitor. Osteoarthritis Cartilage 2002;10:785-91.
33. Gerwin N, Bendele AM, Glasson S, Carlson CS. The OARSI histopathology initiative – Recommendations for histological assessments of osteoarthritis in the rat. Osteoarthritis Cartilage 2010;18 Suppl 3:S24-34.
34. Yu DG, Yu B, Mao YQ, Zhao X, Wang XQ, Ding HF, *et al.* Efficacy of zoledronic acid in treatment of teoarthritis is dependent on the disease progression stage in rat medial meniscal tear model. Acta Pharmacol Sin 2012;33:924-34.
35. Nyman JS, Makowski AJ, Patil CA, Masui TP, O'Quinn EC, Bi X, *et al.* Measuring differences in compositional properties of bone tissue by confocal Raman spectroscopy. Calcif Tissue Int 2011;89:111-22.
36. Lieber CA, Mahadevan-Jansen A. Automated method for subtraction of fluorescence from biological Raman spectra. Appl Spectrosc 2003;57:1363-7.
37. Gupta HS, Schratter S, Tesch W, Roschger P, Berzlanovich A, Schoeberl T, *et al.* Two different correlations between nanoindentation modulus and mineral content in the bone-cartilage interface. J Struct Biol 2005;149:138-48.
38. Oliver WC, Pharr GM. Improved technique for determining hardness and elastic modulus using load and displacement sensing indentation experiments. J Mater Res 1992;7:1564-83.
39. Cox LG, van Donkelaar CC, van Rietbergen B, Emans PJ, Ito K. Decreased bone tissue mineralization can partly explain subchondral sclerosis observed in osteoarthritis. Bone 2012;50:1152-61.
40. Burr DB. The importance of subchondral bone in the progression of osteoarthritis. J Rheumatol Suppl 2004;70:77-80.
41. Karsdal MA, Bay-Jensen AC, Lories RJ, Abramson S, Spector T, Pastoureau P, *et al.* The coupling of bone and cartilage turnover in osteoarthritis: Opportunities for bone antiresorptives and anabolics as potential treatments? Ann Rheum Dis 2014;73:336-48.
42. Englund M. The role of biomechanics in the initiation and progression of OA of the knee. Best Pract Res Clin Rheumatol 2010;24:39-46.
43. Madry H, van Dijk CN, Mueller-Gerbl M. The basic science of the subchondral bone. Knee Surg Sports Traumatol Arthrosc 2010;18:419-33.
44. Botter SM, van Osch GJ, Waarsing JH, Day JS, Verhaar JA, Pols HA, *et al.* Quantification of subchondral bone changes in a murine osteoarthritis model using micro-CT. Biorheology 2006;43:379-88.
45. Botter SM, van Osch GJ, Waarsing JH, van der Linden JC, Verhaar JA, Pols HA, *et al.* Cartilage damage pattern in relation to subchondral plate thickness in a collagenase-induced model of osteoarthritis. Osteoarthritis Cartilage 2008;16:506-14.
46. Botter SM, van Osch GJ, Clockaerts S, Waarsing JH, Weinans H, van Leeuwen JP. Osteoarthritis induction leads to early and temporal subchondral plate porosity in the tibial plateau of mice: An *in vivo* microfocal computed tomography study. Arthritis Rheum 2011;63:2690-9.
47. Anderson-MacKenzie JM, Quasnichka HL, Starr RL, Lewis EJ, Billingham ME, Bailey AJ. Fundamental subchondral bone changes in spontaneous knee osteoarthritis. Int J Biochem Cell Biol 2005;37:224-36.
48. Wachsmuth L, Engelke K. High-resolution imaging of osteoarthritis using microcomputed tomography. Methods Mol Med 2004;101:231-48.
49. Agarwal SC, Stout SD. Bone Loss and Osteoporosis: An Anthropological Perspective. New York, Kluwer Academic/Plenum Publishers: Springer; 2003.
50. Bentolila V, Boyce TM, Fyhrie DP, Drumb R, Skerry TM, Schaffler MB. Intracortical remodeling in adult rat long bones after fatigue loading. Bone 1998;23:275-81.
51. Verborgt O, Gibson GJ, Schaffler MB. Loss of osteocyte integrity in association with microdamage and bone remodeling after fatigue *in vivo*. J Bone Miner Res 2000;15:60-7.
52. Pesesse L, Sanchez C, Henrotin Y. Osteochondral plate angiogenesis: A new treatment target in osteoarthritis. Joint Bone Spine 2011;78:144-9.
53. Pan J, Wang B, Li W, Zhou X, Scherr T, Yang Y, *et al.* Elevated cross-talk between subchondral bone and cartilage in osteoarthritic joints. Bone 2012;51:212-7.
54. Hopwood B, Tsykin A, Findlay DM, Fazzalari NL. Microarray gene expression profiling of osteoarthritic bone suggests altered bone remodelling, WNT and transforming growth factor-beta/bone morphogenic protein signalling. Arthritis Res Ther 2007;9:R100.
55. Nielsen RH, Bay-Jensen AC, Byrjalsen I, Karsdal MA. Oral salmon calcitonin reduces cartilage and bone pathology in an osteoarthritis rat model with increased subchondral bone turnover. Osteoarthritis Cartilage 2011;19:466-73.
56. Sagar DR, Ashraf S, Xu L, Burston JJ, Menhinick MR, Poulter CL, *et al.* Osteoprotegerin reduces the development of pain behaviour and joint pathology in a model of osteoarthritis. Ann Rheum Dis 2014;73:1558-65.
57. Bingham CO 3rd, Buckland-Wright JC, Garnero P, Cohen SB, Dougados M, Adami S, *et al.* Risedronate decreases biochemical markers of cartilage degradation but does not decrease symptoms or slow radiographic progression in patients with medial compartment osteoarthritis of the knee: Results of the two-year multinational knee osteoarthritis structural arthritis study. Arthritis Rheum 2006;54:3494-507.
58. Karsdal MA, Byrjalsen I, Henriksen K, Riis BJ, Lau EM, Arnold M, *et al.* The effect of oral salmon calcitonin delivered with 5-CNAC on bone and cartilage degradation in osteoarthritic patients: A 14-day randomized study. Osteoarthritis Cartilage 2010;18:150-9.
59. Pelletier JP, Roubille C, Raynauld JP, Abram F, Dorais M, Delorme P, *et al.* Disease-modifying effect of strontium ranelate in a subset of patients from the Phase III knee osteoarthritis study SEKOIA using quantitative MRI: Reduction in bone marrow lesions protects against cartilage loss. Ann Rheum Dis 2015;74:422-9.
60. Saag KG. Bisphosphonates for osteoarthritis prevention: "Holy Grail" or not? Ann Rheum Dis 2008;67:1358-9.